ACS APPLIED MATERIALS & INTERFACES

Research Article

www.acsami.org

Host-Mediated Synthesis of Cobalt Aluminate/γ-Alumina Nanoflakes: A Dispersible Composite Pigment with High Catalytic Activities

Anirban Dandapat and Goutam De*

Nano-Structured Materials Division, Central Glass and Ceramic Research Institute, Council of Scientific and Industrial Research, 196, Raja S. C. Mullick Road, Kolkata 700032, India

Supporting Information

ABSTRACT: Cobalt aluminate/γ-alumina ($CoAl_2O_4/\gamma$-Al_2O_3) nanocomposite pigment with mesoporous structure has been synthesized. The method simply involves adsorption of Co^{2+} ion on the surface of a commercially available boehmite (AlOOH) powder followed by the reaction of Co^{2+} and AlOOH at relatively low temperature (500 °C) to obtain $CoAl_2O_4/\gamma$-Al_2O_3 composite nanopowders. The formation of γ-Al_2O_3 from boehmite induces the in situ generation of isostructural $CoAl_2O_4$ (both crystallize as cubic spinel) at such a low temperature. The obtained intense blue powder of optimal composition (53.6 wt % $CoAl_2O_4$ in γ-Al_2O_3) can be dispersed in glycerol and characterized by UV−visible, X-ray diffraction, Raman spectroscopy, TEM, and nitrogen sorption analyses. Raman studies confirm the formation of $CoAl_2O_4$ phase in γ-Al_2O_3. TEM studies reveal the formation of flake shaped (5−10 nm in width and 10−25 nm in length) nanopowders, and these flakes are assembled to form mesoporous structure. The specific surface area, total pore volume and average pore diameter of this powder are estimated to be ∼118 $m^2\ g^{-1}$, 0.1375 $cm^3\ g^{-1}$, and 4.65 nm, respectively. This composite nanopowder has been used as an active catalyst for the decomposition of H_2O_2 at room temperature and the decomposition follows the first order kinetics with rate constant value close to 2.3×10^{-2} min^{-1}. This pigment nanopowder can be reused for several cycles without noticeable degradation of its original catalytic activity.

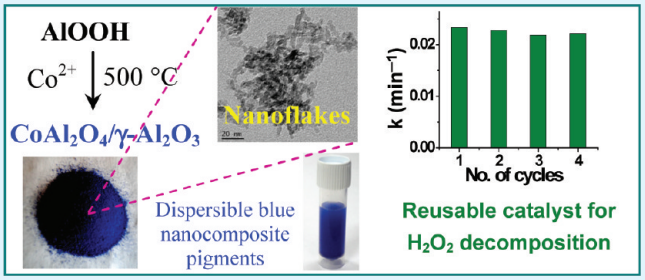

KEYWORDS: *host-mediated synthesis, $CoAl_2O_4/\gamma$-Al_2O_3 composite nanopowder, dispersible pigment, reusable catalyst, self-cleaning pigment*

1. INTRODUCTION

Among the inorganic blue pigments, cobalt aluminate ($CoAl_2O_4$)[1−4] is most attractive because of its excellent thermal, chemical, solar, and atmospheric stabilities with impressive optical,[5,6] dielectric,[7] and sensing[8] properties. The conventional method to synthesize $CoAl_2O_4$ generally requires high temperature (∼1000 °C) and long time.[1−3,9−13] In the literature, there are several routes to prepare cobalt aluminate viz. complexation method,[12] sonochemical technique,[13] solvothermal process,[14] and sol−gel route.[15] Feldmann[4] described the synthesis of blue $CoAl_2O_4$ by two step process. He used the polyol method to obtain purple colored product by refluxing at 180 °C in diethylene glycol followed by heat-treatment at 600 °C to obtain blue colored $CoAl_2O_4$. Recently Rangappa et al[5,6] reported the synthesis of cobalt aluminate nanocrystals under supercritical condition in aqueous medium at ∼400 °C and high pressure. $CoAl_2O_4$ has a cubic spinel structure (Figure 1) with a space group of *Fd*3*m* having lattice constant values 8.1 Å.[16] In cubic spinel structure, Co^{2+} ions occupy the tetrahedral (T_d) sites, whereas Al^{3+} ions are accommodated in octahedral (O_h) sites. It can be noted here that γ-Al_2O_3 has also a cubic spinel structure having same space group (Fd3m) with lattice constant value (7.9 Å) very close to that of $CoAl_2O_4$.[17] Thus the structure of γ-Al_2O_3 can influence the formation of isostructural $CoAl_2O_4$. During the synthesis of Fischer−Tropsch catalyst (Co/γ-Al_2O_3) starting from Co^{2+} salt impregnated

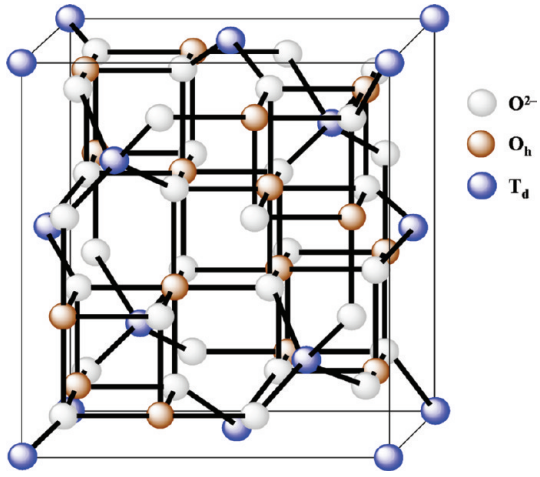

Figure 1. Schematic representation of the cubic spinel structure.

Received: September 20, 2011
Accepted: November 28, 2011
Published: November 28, 2011

γ-Al_2O_3, it was reported that a smaller fraction of non-stoichiometric surface cobalt aluminate can be formed with Co_3O_4 at relatively lower temperature (300−350 °C).[18] More recently Mo et al reported synthesis of $CoAl_2O_4$ from Co^{2+} adsorbed γ-Al_2O_3 powders at very high temperature (~1200 °C).[11]

It is to be noted here that γ-Al_2O_3 could be formed from boehmite precursor at ~400−500 °C.[19] Therefore, in the presence of Co^{2+} ions, it is expected that during the crystallographic conversion of boehmite to γ-Al_2O_3, Co^{2+} ions can be easily occupied into the crystal lattice of γ-Al_2O_3 to form the isostructural $CoAl_2O_4$ at ~400−500 °C. With this idea in mind, we have attempted to synthesize $CoAl_2O_4$ following a simple process from Co^{2+} adsorbed boehmite (AlOOH) powders. Boehmite is known to have orthorhombic layer structure where layers are held together by hydrogen bonds between the hydroxyl groups located in the interlayer space and its overall oxygen lattice is fcc type.[20] The oxygen lattice of γ-Al_2O_3 cubic spinel is built up by a closed packed stacking of oxygen layers and Al^{3+} ions occupy both the O_h and T_d sites (Figure 1). To satisfy the stoichiometry of γ-Al_2O_3 some of the lattice sites remain empty (vacancies). It can be expected that if boehmite is heat-treated at ~500 °C in the presence of Co^{2+}, transformation of the orthorhombic structure of boehmite to cubic spinel will take place with bond breaking where Al^{3+} ions having higher cationic charge would prefer to sit at the O_h positions and Co^{2+} ions can easily enter into the T_d sites of the cubic spinel structure (Figure 1). This is because Al^{3+} ions having higher cationic charge provide greater lattice energy and stability when placed in O_h environment (coordination no. 6) compared to T_d environment (coordination no. 4). So, when Co^{2+} adsorbed boehmite will be heated, the $CoAl_2O_4$ spinel is expected to be formed simultaneously at the same temperature during the formation of isostructural γ-Al_2O_3. This procedure would also produce high surface area mesoporous structure in the final composite materials ($CoAl_2O_4$/γ-Al_2O_3) due to the porous nature of boehmite precursor.

Our aim was also to study the catalytic activity of the $CoAl_2O_4$/γ-Al_2O_3 nanocomposites so that the material can be useful both as pigments and catalyst simultaneously. Although a few groups[21−23] have applied $CoAl_2O_4$ as catalyst in the oxidations of CO, the use of $CoAl_2O_4$ as catalyst is still surprisingly very narrow due to its inert behavior. But, keeping in view of its low cost, environment friendly and nontoxic character,[24] the simultaneous use of $CoAl_2O_4$ as a pigment as well as catalyst is highly admirable. Catalytic decomposition of H_2O_2 is of growing interest due to its wide applications in oxidation and degradation of various kinds of organic pollutants in water and soils.[25−27] Decomposition of H_2O_2 over heterogeneous catalysts such as FeOOH, different forms of Fe_2O_3 and activated carbon have been investigated.[28−32] We observed for the first time that the synthesized $CoAl_2O_4$/γ-Al_2O_3 nanopigment acted as an excellent catalyst to decompose H_2O_2 in aqueous solution at room temperature, and can be reused several cycles without any noticeable degradation of its original catalytic activities.

2. EXPERIMENTAL SECTION

2.1. Materials. AlOOH (P2) was supplied by Condea, Germany. Cobalt chloride and hydrogen peroxide were purchased from Merck. Potassium permanganate was supplied by Sarabhai M chemicals Pvt. Ltd. Cobalt aluminate was bought from Alfa Aesar. Millipore water (~18 MΩ.cm) was used.

2.2. Cobalt Doping in AlOOH Powders. Cobalt was incorporated within AlOOH powders by wet impregnation method.[33] Calculated amount of AlOOH (P2) and aqueous cobalt chloride solution was mixed with stirring for 30 min and then allowed to settle for 12 h. The major portion of the cobalt ions was adsorbed by P2 powders and the supernatant solution became almost colorless. The supernatant solution was filtered off and the resulting solids were dried at 60 °C for 6 h. Four sets of compositions with nominal Co:Al mol ratios of 1:15, 1:8, 1:5 and 1:4 were prepared following the similar procedure. The dried powders were heat-treated to 500 °C for 2 h to obtain $CoAl_2O_4$/γ-Al_2O_3 composite nanopowders. The powders obtained from the composition (Co:Al = 1:5; designated as CA5) was also further heat-treated at 650 and 800 °C with holding time of 2 h at each temperature.

2.3. Characterizations of Co-Doped AlOOH Powders. UV−visible spectrum was obtained by using Cary 50 Scan spectrophotometer. FTIR spectra of the powders were recorded using a Perkin-Elmer 783 spectrometer. Raman spectra of the samples were collected by using Renishaw inVia Raman microspectrometer with 785 nm laser. The powder XRD patterns were recorded on Rigaku SmartLab diffractometer operating at 9 kW with Cu Kα radiation (λ = 1.5405 Å). The surface areas were determined by N_2 sorption analysis at 77.4 K by Quantachrome Autosorb 1 instrument. Prior to measurements the samples were degassed at 300 °C for 12 h with an outgassing pressure of ~0.038 T. The values of specific surface area were determined by multipoint BET method within the range of 0.05−0.35 of relative pressure. The pore size distributions were determined by BJH method from the adsorption bench of the isotherm. Quantitative estimation of Co and Al were carried out by wavelength dispersive X-ray fluorescence (WDXRF) analysis (PANalytical, Model Axios). Transmission electron microscopic (TEM) measurements were carried out using Tecnai G^2 30ST (FEI) operating at 300 kV attached with an energy dispersive X-ray scattering (EDX) unit.

2.4. Catalytic Decomposition of Hydrogen Peroxide. A flask containing hydrogen peroxide (0.02 M) and the studied catalyst (2 g L^{-1}) was shaken during the reaction. When the reaction was in progress, at every 15 min interval, a portion of solution was pipetted out and filtered and then used to determine the remaining concentrations of hydrogen peroxide by permanganate titration method.[31] After the completion of the reaction the powders were separated by centrifugation (5000 rpm/15 min) and subsequently dried at 60 °C for 60 min and then reused.

3. RESULTS AND DISCUSSION

3.1. Composition of the Sample. Visual observation showed that the blue color (due to the formation of $CoAl_2O_4$) of the heat-treated (500 °C) samples gradually intensified with increasing the Co content up to the ratio of Co:Al = 1:5 (CA5). Further increase of Co content (Co:Al = 1:4) yielded black powders at 500 °C due the formation of crystalline Co_3O_4 phase (confirmed by XRD study; see Figure S1 in the Supporting Information) along with $CoAl_2O_4$. As the CA5 powder showed highest catalytic activity[34] with intense blue coloration and dispersibility, this sample was characterized in detail and reported in the subsequent sections. The molar ratio of Co and Al in CA5 sample was checked by WDXRF and found to be very close to 1:5 after averaging the data of 3 analyses. This molar ratio (Co:Al = 1:5) indicated presence of about 53.6 wt % $CoAl_2O_4$ in Al_2O_3 in this sample. The composition of this sample also verified by EDX analysis and found to be very close to that of WDXRF data. This will be discussed in the TEM section.

3.2. Optical Studies. Co^{2+} adsorbed AlOOH powders became deep blue (CA5; Figure 2a) after heat-treating at 500 °C. This blue powder can be dispersed in glycerol. Five wt% dispersion of CA5/500 °C is shown in Figure 2b. UV−visible

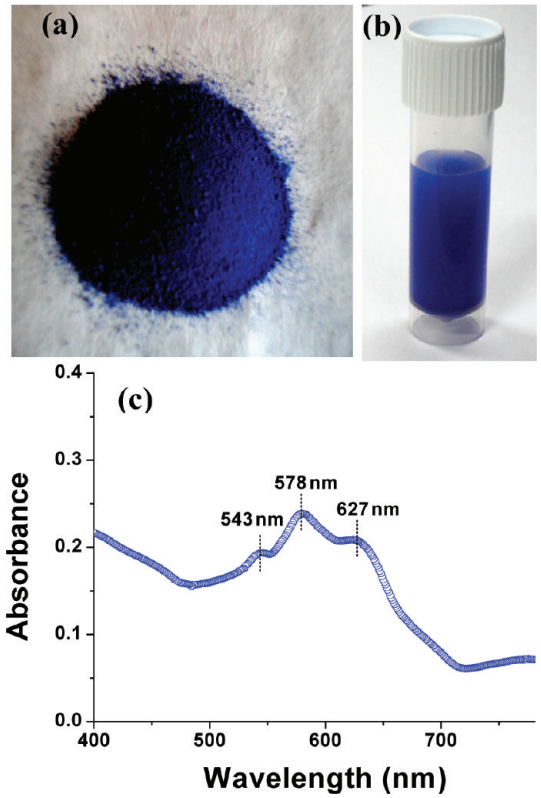

Figure 2. Photos of (a) $CoAl_2O_4/\gamma$-Al_2O_3 composite nanopowder (CA5/500 °C) and (b) 5 wt % dispersion of CA5/500 °C in glycerol; (c) UV−visible absorption spectrum of 15 times diluted solution of b.

absorption spectrum of the 15 times diluted solution of this dispersion is shown in Figure 2c. It shows three absorptions (triple band) at around 543, 578, and 627 nm typically for Co^{2+} ions present in a T_d ligand field with $3d^7$ configurations. The triple band can be attributed to $^4A_2(F) \rightarrow {}^4T_1(P)$ transitions[15,35] arrising from the Jahn−Teller distortion of the T_d structure.[36] Thus, the UV−visible study at the first instance confirmed the formation of cobalt aluminate.

3.3. Raman Studies. It is known that $CoAl_2O_4$ spinel (Figure 1) belonging to the space group Fd3m (O_h^7) should show five Raman active bands ($A_{1g} + E_g + 3F_{2g}$).[37,38] Raman spectrum of the blue nanopowder CA5 (heat-treated at 500 °C) is presented in Figure 3 that shows strong Raman bands at 196, 480, 519, 619, and 690 cm^{-1}. The band at 690 cm^{-1} can be assigned to A_{1g} species in O_h^7 spectroscopic symmetry, whereas 619, 519, and 196 cm^{-1} peaks are assigned to three F_{2g} symmetry species and the bands at 480 cm^{-1} is due to E_g symmetry. Two very weak additional bands appearing near 770 and 269 cm^{-1} (Figure 3) may be due to lower crystal symmetry in the spinel structure.[37,38] Raman spectrum of γ-Al_2O_3 powders prepared from boehmite by heat-treating at 500 °C is also presented in the Figure 3 to show the absence of such Raman active bands in case of γ-Al_2O_3. Therefore, appearance of the characteristic Raman peaks for CA5/500 °C powder confirmed the formation of cobalt aluminate.

3.4. XRD Characterization. XRD patterns of the CA5 powders heated at different temperatures were recorded and presented in Figure 4 along with the undoped γ-Al_2O_3. XRD pattern of the blue powder (CA5/500 °C) is seemed to be

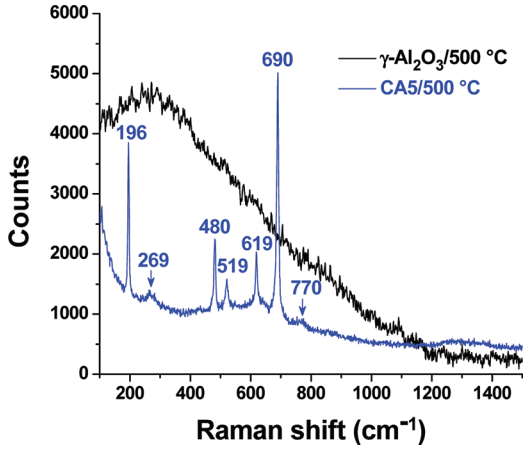

Figure 3. Raman spectrum of $CoAl_2O_4/\gamma$-Al_2O_3 composite nanopowder (CA5/500 °C) and boehmite derived γ-Al_2O_3 powders heat-treated at 500 °C in a similar fashion.

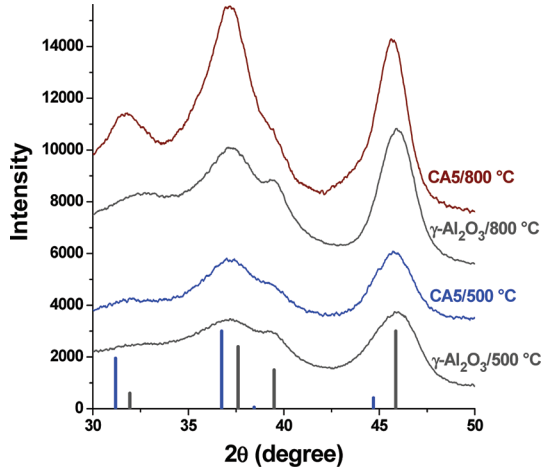

Figure 4. XRD patterns of $CoAl_2O_4/\gamma$-Al_2O_3 composite nanopowder (CA5) heat-treated at 500 and 800 °C. The patterns of the corresponding boehmite derived γ-Al_2O_3 powders heat-treated in a similar fashion are also shown for comparison. *Y*-axis scale has been shifted for clarity.

similar to that of γ-Al_2O_3. This is expected because both $CoAl_2O_4$ and γ-Al_2O_3 crystallize as cubic spinel structure (Figure 1) with a small difference in lattice constant values.[16,17] Further, nanocrystalline nature of sample makes the X-ray line broadening. Therefore from XRD analysis it is difficult to distinguish between the $CoAl_2O_4$ and γ-Al_2O_3 phases because of their structural similarity. It has been observed that the relative intensities of peaks at around 37 and 39.5° 2θ of undoped γ-Al_2O_3 (heat-treated at 500 °C) (Figure 4) match well with the values given in the literature (JCPDS # 00−010−0425).[39] Careful observation of the XRD pattern of CA5 powder heat-treated at 500 °C showed (Figure 4) that the relative intensity of ∼37° 2θ peak was more than that of the ∼39.5° peak. As $CoAl_2O_4$ has the 100 intensity peak at ∼36.74° 2θ (JCPDS# 00−044−0160), the increase in 37° 2θ peak intensity can be considered as the contribution from $CoAl_2O_4$ species. This can be further understood by heat-treating CA5/500 °C at higher temperature (800 °C) to enhance the crystallinity of $CoAl_2O_4$. As expected, the 800 °C heat-treated sample showed further enhancement of 37° 2θ peak intensity

dx.doi.org/10.1021/am201283c | ACS Appl. Mater. Interfaces 2012, 4, 228−234

(Figure 4) suggesting more crystalline nature of $CoAl_2O_4$. So, XRD studies revealed existence of nanocrystalline $CoAl_2O_4$ in the CA5 sample. The crystallinity is however lower in case of 500 °C sample compared to the 800 °C treated powder.

3.5. Nitrogen Sorption Analysis. N_2 sorption analysis of the nanopowders was performed to measure the specific surface area and average pore diameter of the porous powders. Adsorption-desorption isotherms presented in Figure 5 showed a typical type IV isotherm (Figure 5a) indicating the presence of mesoporous structure.[40,41] The pore size distribution obtained from the adsorption branch of the isotherm is shown in Figure 5b confirming the mesoporous structure of the synthesized blue nanocomposites CA5 obtained at 500 °C. The multipoint BET surface area, total pore volume and average pore diameter of the CA5/500 °C powders were 118.3 $m^2\ g^{-1}$, 0.1375 $cm^3\ g^{-1}$ and 4.65 nm, respectively. The multipoint BET surface area values of the further heat-treated CA5/650 °C and CA5/800 °C samples were also estimated and found to be 102.1 and 70.2 $m^2\ g^{-1}$, respectively.

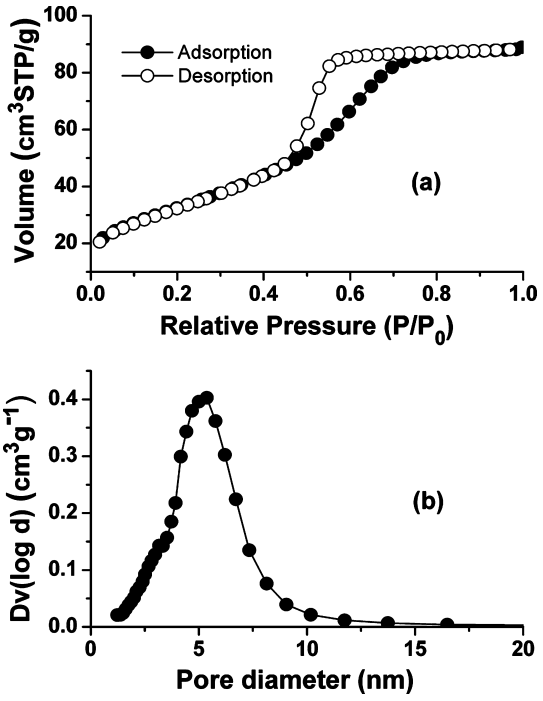

Figure 5. N_2 sorption analysis of the mesoporous $CoAl_2O_4/\gamma$-Al_2O_3 composite nanopowder (CA5/500 °C): (a) isotherms and (b) corresponding pore size distribution obtained from the adsorption bench of isotherm.

3.6. TEM Studies. STEM image of the CA5/500 °C powders is shown in Figure 6a. The quantitative EDX analysis of the sample was performed to estimate the atomic ratios of Co:Al as well as to check the uniformity of the sample. For this purpose, three different points of the samples were analyzed by focusing the nanoprobe (the positions are marked in the Figure 6a). EDX patterns obtained from all these positions show the presence of mainly Co, Al, and O. Small amount of Cl peak (from precursor cobalt chloride) and strong Cu peaks (from the TEM-grid) are also observed. A representative EDX spectrum is shown in Figure 6b. The Co:Al atomic ratios (indicated with Figure 6 as a tabular format) estimated from all these three different positions showed quite uniformity of the sample with an average Co:Al value of 1:5.3 which is close to the estimated value by WDXRF. TEM analysis of the sample is presented in Figure 7. TEM images (Figure 7a, b) show that CA5/500 °C has nanoflake-like structure (~10–25 nm in length and ~5–10 nm in diameter). These nanoflakes are aggregated to form a mesoporous structure which can be understood from Figure 7b. SAED pattern (Figure 7c) shows the presence of planes corresponding to γ-Al_2O_3 and $CoAl_2O_4$. High-resolution TEM image and corresponding FFT analysis (Figure 7d) show the lattice spacings of 1.97 Å and 2.44 Å those can be indexed for the 100 intensity peaks of γ-Al_2O_3 [(400) plane] and $CoAl_2O_4$ [(311) plane], respectively.

3.7. Catalytic Activities. CA5/500 °C powder is found to be very active catalyst for the decomposition of hydrogen peroxide at pH 7.[34] It can be noted here that metal oxide-catalyzed decomposition of hydrogen peroxide occurred

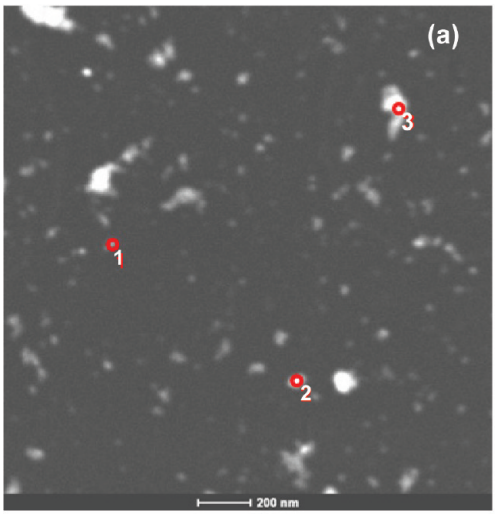

Position	Co:Al	Co:Al (average)
1	1:6.5	1:5.3
2	1:5.1	
3	1:4.3	

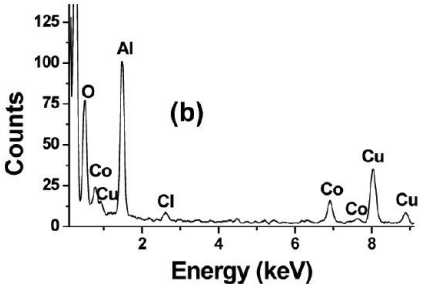

Figure 6. Quantitative elemental analysis of CA5/500 °C sample obtained from three different points using STEM-EDX analysis. (a) STEM image showing the analyzed three different points with marking (1–3) along with the compositions in the tabular form and (b) a representative EDX pattern obtained from the point marked as 2.

dx.doi.org/10.1021/am201283c | ACS Appl. Mater. Interfaces 2012, 4, 228–234

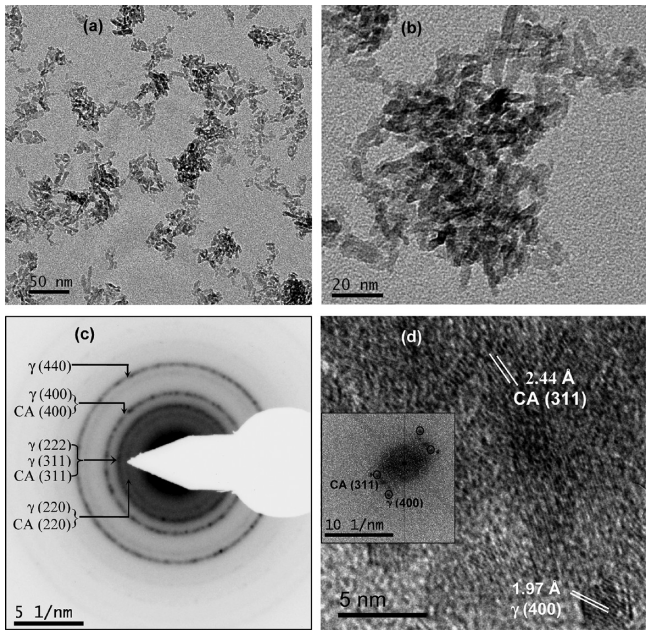

Figure 7. (a, b) TEM studies of the $CoAl_2O_4/\gamma$-Al_2O_3 composite nanopowder (CA5/500 °C) with different magnifications; (c) SAED pattern obtained from Figure 7(a), and (d) high resolution TEM image of the nanopowder and the FFT pattern (inset) showing spots corresponding to CA (311) and γ-Al_2O_3 (400). In the figure, γ and CA stand for γ-Al_2O_3 and cobalt aluminate, respectively.

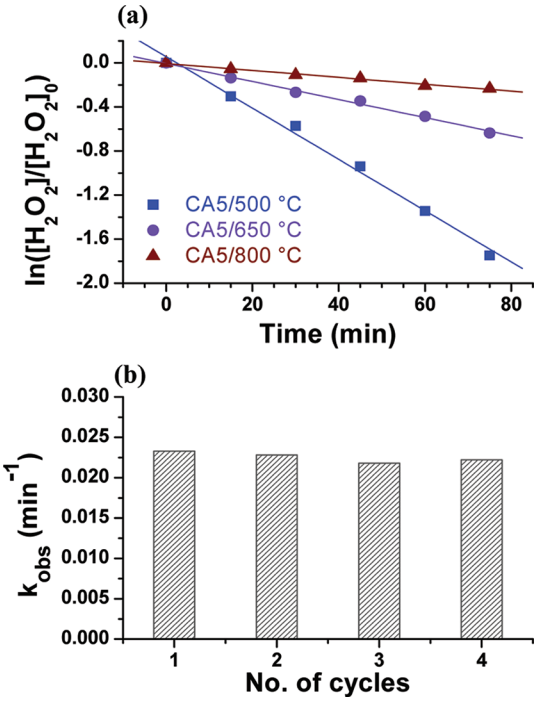

Figure 8. (a) Plot of $\ln([H_2O_2]/[H_2O_2]_0)$ vs time for the decomposition of hydrogen peroxide in presence of CA5/500 °C, CA5/650 °C and CA5/800 °C samples at room temperature and (b) rate constant values (k_{obs}) of the catalytic decomposition of hydrogen peroxide in four consecutive cycles using the same catalyst CA5/500 °C.

according to the following mechanism[42]

$$[\equiv M - O]OH + H_2O_2 \rightarrow [\equiv M - O]OH - H_2O_2 \leftrightarrow [\equiv M - O] + {}^{\bullet}OOH + H_2O \quad (1)$$

$$[\equiv M - O] + {}^{\bullet}OOH \rightarrow [\equiv M - O]H + O_2 \quad (2)$$

$$[\equiv M - O]H + H_2O_2 \rightarrow [\equiv M - O]OH + H_2O \quad (3)$$

In the presence of metal oxide, the decomposition of hydrogen peroxide is expected to follow a first order rate law kinetics with respect to H_2O_2, i.e., $-d[H_2O_2]/dt = k_{obs}[H_2O_2]$[42,43] and thus $\ln([H_2O_2]/[H_2O_2]_0) = -k_{obs}t$, where k_{obs} is the observed first-order rate constant, and $[H_2O_2]$ and $[H_2O_2]_0$ are the concentrations of hydrogen peroxide in the solution at any time "t" and time "zero" respectively. We have carried out the catalytic decomposition of aqueous H_2O_2 solution (0.02 M) by using the $CoAl_2O_4/\gamma$-Al_2O_3 composite nanopowder (CA5) heat-treated at 500 °C. The linear plot of $\ln([H_2O_2]/[H_2O_2]_0)$ vs time (shown in Figure 8a) confirmed the first-order kinetics and the calculated value of k_{obs} was estimated to be 2.33×10^{-2} min^{-1}. When the reaction was completed, the catalyst powder was centrifuged and dried at 60 °C for 60 min and then reused. The reaction carried out with these used catalyst showed similar catalytic activities like the original sample. The k_{obs} values obtained from four consecutive cycles using the same catalyst are shown in Figure 8b. We have checked the reaction by using γ-Al_2O_3 (blank sample prepared in a similar way by heat-treating P2 grade boehmite at 500 °C) and found that it was inactive toward the degradations of H_2O_2, confirming the fact that $CoAl_2O_4$ present in γ-Al_2O_3 is actually responsible for this catalytic process. We have also carried out the reaction in presence of commercially available cobalt aluminate (Alfa Aesar) powder. In this case also, the degradation of H_2O_2 was insignificant within the experimental period of time (75 min). The commercially available cobalt aluminate powder was also analyzed by XRD, FTIR and N_2 sorption analysis. XRD pattern (see Figure S2 in the Supporting Information) showed highly crystalline nature of the powders and the peaks are well matched with JCPDS card # 00–044–0160. FTIR spectra of the commercially available crystalline $CoAl_2O_4$ showed very weak band near ~3200–3600 cm^{-1} region due to OH stretching vibrations,[13] whereas $CoAl_2O_4/\gamma$-Al_2O_3 composite nanopowder (CA5/500 °C) showed strong OH stretching related peaks around 3440 cm^{-1} as shown in Figure S3 in the Supporting Information. The surface area of commercial powder was estimated to be 0.93 m^2g^{-1} revealing the nonporous characteristics. According to the reaction mechanisms shown in eqs 1–3, surface hydroxyl groups play an important role during the decomposition process. Therefore, it is expected that inadequate numbers of surface hydroxyl groups and nonporous nature of the commercially available $CoAl_2O_4$ powders made them inactive toward the catalytic decomposition of H_2O_2. To confirm the effect of surface hydroxyl (OH) groups and specific surface area, we also studied the catalytic activities of the CA5 powders after heat-treating them at 650 and 800 °C. It was observed that the k_{obs} values were decreased to 0.82×10^{-2} and 0.31×10^{-2} min^{-1} in the cases of CA5/650 °C and CA5/800 °C samples, respectively as shown in Figure 8a. As expected, the FTIR studies confirmed gradual decrease of OH groups (see Figure S3 in the Supporting Information) when the CA5 powders were heated to higher temperatures, and the corresponding surface area values were also decreased from 118.0 m^2 g^{-1} (CA5/500 °C) to 102.1 and

dx.doi.org/10.1021/am201283c | ACS Appl. Mater. Interfaces 2012, 4, 228–234

70.2 m^2 g^{-1} for CA5/650 °C and CA5/800 °C samples, respectively. So the main reason of higher catalytic property of the CA5/500 °C composite nanopowder was due to its high surface area and the presence of large amount of surface OH groups. Increase of heat-treatment temperature reduced the concentration of OH and surface area, and consequently the samples showed less catalytic activities. A comparison of catalytic activities of CA5/500 °C powder with other reported work is presented in Table S2 in the (Supporting Information). The normalized rate constant (k_{nor})[44] value for the decomposition of H_2O_2 as listed in Table S2 in the Supporting Information, shows that CA5/500 °C has a slight less activity compared to a very recent report using high surface area γ-Fe_2O_3.[32] Except this report CA5/500 °C shows higher[28−30] and comparable[31] activity with the other reported catalysts (see Table S2 in the Supporting Information). Another important observation is the reusability of CA5/500 °C as catalyst. So the developed CA5/500 °C nanocomposite powders can find important applications because of its simultaneous use as a pigment with high catalytic property.

As we have thought and discussed in the introduction section, $CoAl_2O_4$ has been generated with γ-Al_2O_3 after the heat-treatment of Co^{2+} adsorbed boehmite (P2) powders at relatively low temperature (~500 °C). During the conversion of boehmite to γ-Al_2O_3, the isostructural $CoAl_2O_4$ was also formed simultaneously by replacing the T_d Al^{3+} with Co^{2+} ions. So, the synthesis of nano $CoAl_2O_4$ with γ-Al_2O_3 has been successfully accomplished at relatively low temperature. This $CoAl_2O_4$/γ-Al_2O_3 composite nanopowder pigments synthesized by this new technique not only save energy (low temperature) but also produces intense coloration, nanoparticulate mesoporous structure with high surface area, and active surface hydroxyl groups suitable for the decomposition of H_2O_2 with reusability.

4. CONCLUSIONS

We have reported a simple, facile, and scalable synthetic procedure for the preparation of high surface area $CoAl_2O_4$/γ-Al_2O_3 composite nanopowder which can be used as self-cleaning blue pigments. In this procedure, a stable cobalt aluminate has been synthesized at low temperature (~500 °C) compared to the conventional high temperature methods. It can be concluded that the conversion of boehmite to γ-Al_2O_3 facilitated the formation of isostructural $CoAl_2O_4$ at relatively low temperature. Another benefit of achieving high surface area with active surface hydroxyls is due to the use of porous boehmite powder as precursor. We have shown for the first time that this $CoAl_2O_4$ spinel composite can act as an efficient catalyst for the decomposition of H_2O_2 to release oxygen that may oxidize a wide range of organic and inorganic pollutants. It may be possible to use this CA5 powder with paints in the walls of industrial wastewater treatment chambers, where catalytic decomposition of H_2O_2 would facilitate waste decomposition. To paint the buildings, this dispersible CA5 powders can be used as pigment which will help to keep clean the wall through removal of fungus deposition by simply spraying the nontoxic dilute H_2O_2 as and when required. Therefore, these nano blue pigments can find important applications owing to their stability, dispersibility, high surface area and catalytic performances with reusability. The synthetic strategy shown in this work can be used to prepare many other similar composite nanopowder of technological importance.

■ ASSOCIATED CONTENT

Supporting Information

XRD patterns of the composite powders with nominal Co:Al mol ratio of 1:4 (Figure S1) and commercially available $CoAl_2O_4$ (Figure S2), FTIR spectral evolution of $CoAl_2O_4$/γ-Al_2O_3 nanocomposites (CA5) with respect to the heat-treatment temperatures and commercially available $CoAl_2O_4$ (Figure S3), rate constant values (k_{obs}) for the decomposition of H_2O_2 using different compositions with nominal Co:Al mol ratios of 1:15, 1:8, 1:5 and 1:4 (Table S1), and comparative k_{obs} values by different types of catalysts (Table S2). This material is available free of charge via the Internet at http://pubs.acs.org.

■ AUTHOR INFORMATION

Corresponding Author

*Tel: +91 33 24733469/96, ext. 3403. Fax: 91-33-24730957. E-mail: gde@cgcri.res.in.

■ ACKNOWLEDGMENTS

The work was financially supported by the Department of Science and Technology (DST), Government of India (Project SR/S5/NM-17/2006) and the Council of Scientific and Industrial Research (CSIR), India (Project NWP051). A.D. thanks CSIR, India for providing a fellowship.

■ REFERENCES

(1) Lin, C.; Li, Y.; Yu, M.; Yang, P.; Lin, J. *Adv. Funct. Mater.* **2007**, *17*, 1459−1465.
(2) Vogt R.; Brückner, H. D. Interference Pigments having a blue mass tone. U.S. Patent No. 6 238 471 B1, May 29,2001.
(3) Cavalcante, P. M. T.; Dondi, M.; Guarini, G.; Raimondo, M.; Baldi, G. *Dyes Pigm.* **2009**, *80*, 226−232.
(4) Feldmann, C. *Adv. Mater.* **2001**, *13*, 1301−1303; *Adv. Funct. Mater.* **2003**, *13*, 101−107.
(5) Rangappa, D.; Naka, T.; Kondo, A.; Ishii, M.; Kobayashi, T.; Adschiri, T. *J. Am. Chem. Soc.* **2007**, *129*, 11061−11066.
(6) Rangappa, D.; Ohara, S.; Naka, T.; Kondo, A.; Ishii, M.; Adschiri, T. *J. Mater. Chem.* **2007**, *17*, 4426−4429.
(7) Ummartyotin, S.; Sangngern, S.; Kaewvilai, A.; Koonsaeng, N.; Manuspiya, H.; Laobuthee, A. *J. Sustainable Energy Environ.* **2009**, *1*, 31−37.
(8) Michel, C. R. *Sens. Actuators B* **2010**, *147*, 635−641.
(9) Meyer, F.; Hempelmann, R.; Mathur, S.; Veith, M. *J. Mater. Chem.* **1999**, *9*, 1755−1763.
(10) Suzuki, T.; Nagai, H.; Nohara, M.; Takagi, H. *J. Phys.: Conden. Matter.* **2007**, *19*, 145265.
(11) Mo, L.; Fei, J.; Huang, C.; Zheng, X. *J. Mol. Catal. A: Chem.* **2003**, *193*, 177−184.
(12) Mindrua, I.; Marinescua, G.; Gingasua, D.; Patrona, L.; Ghicab, C.; Giurginca, M. *Mater. Chem. Phys.* **2010**, *122*, 491−497.
(13) Chen, Z.; Shi, E.; Li, W.; Zheng, Y.; Zhong, W. *Mater. Lett.* **2002**, *55*, 281−284.
(14) Lv, W.; Qiu, Q.; Wang, F.; Wei, S.; Liu, B.; Luo, Z. *Ultrason. Sonochem.* **2010**, *17*, 793−801.
(15) Zayat, M.; Levy, D. *Chem. Mater.* **2000**, *12*, 2763−2769.
(16) Tielens, F.; Calatayud, M.; Franco, R.; Recio, J. M.; Pérez-Ramírez, J.; Minot, C. *J. Phys. Chem. B* **2006**, *110*, 988−995.
(17) Maglia, F.; Gennari, S.; Buscaglia, V. *J. Am. Ceram. Soc.* **2008**, *91*, 283−290.
(18) Jongsomjit, B.; Panpranot, J.; Goodwin, J. G. *J. Catal.* **2001**, *204*, 98−109.
(19) Zhang, Z.; Pinnavaia, T. J. *J. Am. Chem. Soc.* **2002**, *124*, 12294−12301.
(20) Krokidis, X.; Raybaud, P.; Gobichon, A. E.; Rebours, B.; Euzen, P.; Toulhoat, H. *J. Phys. Chem. B* **2001**, *105*, 5121−5130.

(21) Thormählen, P.; Fridell, E.; Cruise, N.; Skoglundh, M.; Palmqvist, A. *Appl. Catal. B: Env.* **2001**, *31*, 1−12.
(22) Zarkov, V.; Mehandjiev, D. *Appl. Catal., A* **1993**, *94*, 161−166.
(23) Baker, J. E.; Burch, R.; Yuqin, N. *Appl. Catal.* **1991**, *73*, 135−152.
(24) Stopford, W.; Turner, J.; Cappellini, D.; Brock, T. *J. Environ. Monit.* **2003**, *5*, 675−680.
(25) Luo, W.; Zhu, L.; Wang, N.; Tang, H.; Cao, M.; She, Y. *Environ. Sci. Technol.* **2010**, *44*, 1786−1791.
(26) Yang, S.; He, H.; Wu, D.; Chen, D.; Ma, Y.; Li, X.; Zhu, J.; Yuan, P. *Ind. Eng. Chem. Res.* **2009**, *48*, 9915−9921.
(27) Dore, M. *Water Res.* **1990**, *24*, 973−982.
(28) Lin, S. H.; Gurol, M. *Environ. Sci. Technol.* **1998**, *32*, 1417−1423.
(29) Huang, H. H.; Lu, M. C.; Chen, J. N. *Wat. Res.* **2001**, *35*, 2291−2299.
(30) Huang, H. H.; Lu, M. C.; Chen, J. N.; Lee, C. T. *Chemosphere* **2003**, *51*, 935−943.
(31) Hermanek, M.; Zboril, R.; Medrik, I.; Pechousek, J.; Gregor, C. *J. Am. Chem. Soc.* **2007**, *129*, 10929−10936.
(32) Hermanek, M.; Hermankova, P.; Pechousek, J. *J. Mater. Chem.* **2010**, *20*, 3709−3715.
(33) Espinoza, R. L.; Jothimurugesan, K.; Jin, Y.; Ortego, J. D.; Fjare, K. A.; Ortego, B. C. Stabilized Boehmite-Derived Catalyst Support, Catalysts, Methods of Making and Using. U.S. Patent No. 7 341 976 B2, March 11, 2008.
(34) Among the different compositions with nominal Co:Al mol ratios from 1:15 to 1:4, the powders with the ratio 1:5 (CA5/500 °C) showed the highest catalytic activity (see Table S1 in the Supporting Information). The activity of the powders containing the highest Co content (Co:Al = 1:4) was found to decrease probably due to the formation of Co_3O_4.
(35) Habra, N. E.; Crociani, L.; Sada, C.; Zanella, P.; Casarin, M.; Rossetto, G.; Carta, G.; Paolucci, G. *Chem. Mater.* **2007**, *19*, 3381−3386.
(36) Bambord, C. R. *Phys. Chem. Glasses* **1962**, *3*, 189−202.
(37) Casado, G. P.; Rasines, I. *J. Solid State Chem.* **1984**, *52*, 187−190.
(38) Bouchard, M.; Gambardella, A. *J. Raman Spectrosc.* **2010**, *41*, 1477−1485.
(39) Dandapat, A.; Jana, D.; De, G. *ACS Appl. Mater. Interface* **2009**, *1*, 833−840.
(40) Nakahira, A.; Kubo, T.; Yamasaki, Y. *ACS Appl. Mater. Interface* **2010**, *2*, 1136−1140.
(41) Dandapat, A.; De, G. *J. Mater. Chem.* **2010**, *20*, 3890−3894.
(42) Do, S. H.; Batchelor, B.; Lee, H. K.; Kong, S. H. *Chemosphere* **2009**, *75*, 8−12.
(43) Lousada, C. M.; Jonsson, M. *J. Phys. Chem. C* **2010**, *114*, 11202−11208.
(44) Jana, D.; Dandapat, A.; De, G. *Langmuir* **2010**, *26*, 12177−12184.